Chemistry Africa (2022) 5:293–304
https://doi.org/10.1007/s42250-022-00327-2

ORIGINAL ARTICLE

Kinetic and Thermodynamic Study of the Photo Catalytic Degradation of Methylene Blue (MB) in Aqueous Solution Using Cadmium Sulphide (CdS) Nanocatalysts

Sundas Ali[1] · F. Akbar Jan[1] · Rahat Ullah[1] · Wajidullah[1] · Naimat Ullah[2]

Received: 6 December 2021 / Accepted: 24 January 2022 / Published online: 4 February 2022

Abstract
Cadmium sulphide (CdS) nanoparticles (NPs) were synthesized through hydrothermal method and characterized by UV–Vis spectroscopy, X-ray diffraction (XRD), energy dispersive X-ray analysis (EDX), scanning electron microscopy (SEM), Fourier transform infrared spectroscopy (FTIR) and thermo gravimetric analysis (TGA). The band gap value of CdS nanoparticles was found to be 2.38 eV. Crystalline aggregates with hexagonal pattern of CdS were shown by SEM and XRD analysis. The TGA study revealed that the synthesized CdS nanomaterials were much stable to temperature and only 6.54% of the total loss occurred during heating range (25–600 °C). The degradation of methylene blue over CdS nanocatalyst followed second order kinetics. The activation energy calculated was 9.043 kJ mol^{-1}. More than 93% dye was degraded at the time interval of 160 min. High degradation of dye was found at low concentration (10 ppm) and at optimal dosage of the catalyst (0.03 g). The rate of MB dye degradation was found to be increases with increase in temperature and pH of the medium. The recyclability study showed that CdS nanoparticles could be reused for the degradation of the given dye.

Keywords Methylene blue dye · CdS NPs · Kinetic and thermodynamic study · Recycled catalyst

1 Introduction

Water is most vital for human beings and due to industrialization and urbanization water quality has been deteriorated thus causing negative impacts on humans and other living organisms. Agriculture, food production as well as economy is also affected by low water quality. Many industries such as paper and printing, lather, textile and cosmetics give organic dyes and pigments to the water bodies and thus render unfit for drinking and other uses [1]. The dyes are colored compounds that prevent sunlight penetration into the water stream, consequently reducing the photosynthetic reactions. Most of the dyes are threat to human beings and animals even cause malignant neoplastic disease [2]. Methylene blue (MB) is one of the industrial dyes that is highly detrimental to the ecosystem, animals and human beings [3]. Various techniques like ozonization, chemical coagulation, oxidation, electrolysis and biodegradation have been used to remove dyes from wastewater. However, these methods are unable to reduce the concentration of the contaminants to the desired levels [4]. Advanced oxidation process (AOP) is an emerging technique that use hydroxyl radicals (HO·) formation, which exhibits strong oxidation capacity ($E_0 = 2.76$ V) leading to the complete mineralization of organic pollutants. These methods including Fenton ($Fe^{2+} + H_2O_2$), photo-Fenton (solar light + Fenton), ozone (O_3), sonolysis (ultrasounds), electrolysis (electrodes + current), photolysis ($UV + H_2O_2$) and photocatalysis (light + catalyst) offers no further requirement for secondary disposal [5–7].

Absorption of photons with energy larger than the band gap of a photo catalyst, second the generation, separation, migration or recombination of electron–hole pairs and finally the redox reactions occurring at the photo catalyst surface are the three steps that are involved in photo catalysis [8].

Due to an empty conduction band and crammed valence band conducting metals (such as ZnO, Fe_2O_3, CdS, and ZnS) can act as sensitizers for light-induced

✉ F. Akbar Jan
fazal_akbarchem@yahoo.com

[1] Department of Chemistry, Bacha Khan University Charsadda, Charsadda 24420, Khyber-Pakhtunkhwa, Pakistan

[2] Department of Chemistry, Qauid-i-Azam University Islamabad, Islamabad 45320, Pakistan

redox-processes [9]. As compared to metal oxides sulfidation of metals has been proven to suppress reactions with water and improve the reactivity and selectivity for organics pollutants. A combination of hydrophobicity and enhanced electron transfer is touted as the main benefit of metals sulfidation, and this was recently confirmed using electrochemical tests and water contact angle measurements [10]. However, these characterizations are both bulk analyses, so it is unclear if the reactive sites are metal or S sites and how sulfur affects the charge density distribution of metal at an atomistic level. However metal sulphide afford the hydrogen evolution reaction (HER) in water, [11] which involves the generation of atomic H (Volmer reaction) via electron transfer from the materials to water and its subsequent combination to form H_2 (Tafel or Heyrovsky reaction) on a metal surface. Although previous studies have shown that H_2, atomic H, and direct electron transfer are all capable of degrading pollutants [12]. Cadmium sulfide (CdS) has promising applications in photoluminescent, electroluminescent and photoconductive devices due to having a narrow band gap of 2.42 eV [13]. Owing to their unique physicochemical properties such as good permeability, high specific surface area and special optical/electrical/magnetic properties, CdS has received particular attention in recent years [14]. Keeping in view the hazards associated with dyes in the aqueous system and importance of CdS nanomaterials a study was designed to synthesize and characterized CdS nanoparticles. Kinetic and thermodynamic study of the effects of various parameters on photo degradation was also the aims of the present study.

2 Experimental

2.1 Apparatus

UV–visible spectrophotometer Model Shimadzu UV-1800, Japan was used for all absorbance measurements. Perkin Elmer FTIR spectrometer version 10.4.00 was used for identification of the functional groups. For pH measurements, Elico (model IL-610) digital pH meter was used. TGA analysis was performed with Shimadzu TGA-50/50H. All the analysis were performed in Advance Research Lab (ARL) Department of Chemistry Bacha Khan University Charsadda. XRD, SEM and EDX analysis of the synthesized materials were carried out in Quaid-i-Azam University Islamabad.

2.2 Synthesis of CdS Nanoparticles

CdS NPs were synthesized through hydrothermal method. In this typical synthesis 15 mL (0.1 M) of each Cd $(NO_3)_2{\cdot}4H_2O$ (cadmium nitrate) and $Na_2S{\cdot}9H_2O$ (sodium sulfide)solutions were taken in a beaker. The mixed solution was stirred at room temperature for about 10 min. Then the mixture was transferred to 50 ml autoclave and was placed in a muffle furnace for 14 h at 200 °C. After heating the reaction mixture, it was centrifuged and washed four times with water. The final product was dried at 50 °C for 5 h. Fig. 1 is the schematic diagram for the synthesis of CdS NPs.

2.3 Preparation of the Dye Solution

Stock solution (500 ppm) of methylene blue dye was prepared in distilled water. Using dilution formula given in

Fig. 1 Flow sheet diagram for the synthesis of CdS nanoparticles

Eq. (1), the working solutions of different concentration were prepared accordingly.

$$M_1V_1 = M_2V_2 \quad (1)$$

2.4 Photocatalytic Degradation of the Dye

The activity of CdS nanoparticles was evaluated in the degradation of methylene blue in aqueous solution. The degradation was carried out in UV-light. The λ_{max} of methylene blue was 668 nm and this was used as a monitor wavelength for photo degradation.

Upon addition of an appropriate amount of photo catalyst (CdS, NPs) the dye solution was stirred for 30 min in the dark to establish adsorption/desorption equilibrium before the photo degradation reaction. During experiments in locally designed equipment the light source (UV-light) was placed 15 cm away from the surface of the solution. The catalyst was removed by centrifugation and the dye degradation was checked at various interval of time using UV–visible spectrometer. Percent degradation of the dye was calculated using the following relation (Eq. 2)

$$D(\%) = \frac{C_0 - C_t}{C_0} \times 100, \quad (2)$$

where C_0 and C_t represents concentrations of MB at time 0 mint and t (s) respectively.

3 Results and Discussion

3.1 UV–Visible Spectroscopic Studies

UV–Vis spectroscopy was performed to observe the maximum absorbance of CdS nanoparticles. The wavelength was employed in the range of 200–800 nm. CdS NPs showed maximum absorbance at 496 nm as shown in Fig. 2 and the band gap was calculated by using Tauc plot given in Eq. 3.

$$(\alpha h\upsilon)^{1/n} = \beta(h\upsilon - Eg), \quad (3)$$

where "α" represent the absorption coefficient, "hυ" is the photon energy, "Eg" show the band gap and value of "n" depends on transition involved where n can have values 1/2, 2, 3/2, 3 related to direct allowed, indirect allowed, direct forbidden and indirect forbidden transitions respectively. CdS nanoparticles show direct allowed transitions[15]. To calculate the value of band gap, graph was plotted $(\alpha h\upsilon)^2$ vs hυ and the straight line obtained was extrapolated to zero absorption co-efficient so that it encountered the x-axis. The band gap value (Fig. 3) of CdS was found to be 2.38 eV.

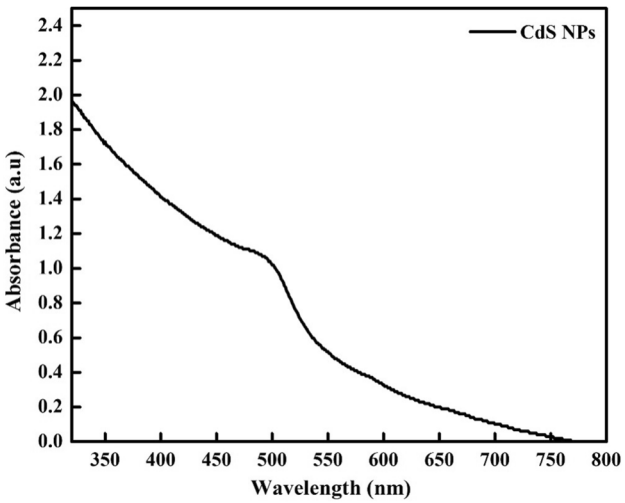

Fig. 2 UV–Vis spectrum of CdS nanoparticles

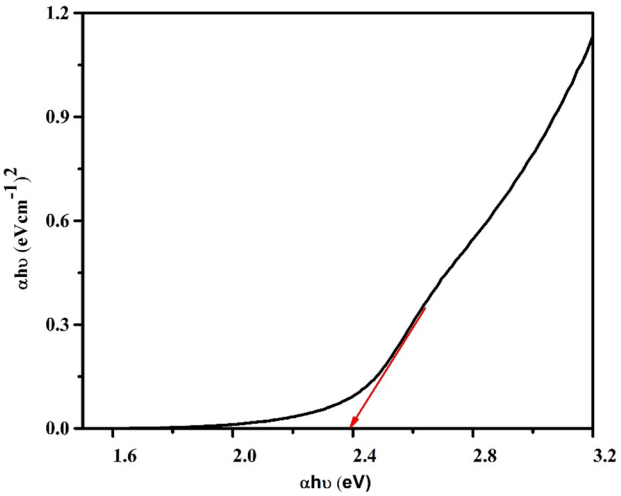

Fig. 3 Tauc plot of of CdS nanoparticles

3.2 XRD Studies

X-rays diffraction powder analysis was carried out to investigate the crystallinity, crystallite size, and phase of nanoparticles. There is no extra peak which indicates the purity of the synthesized NPs [16]. XRD pattern (Fig. 4) showed the hexagonal pattern of CdS. The diffraction peaks were observed at 24.840°, 26.370°, 30.47°, 43.79°, 51.87°, 54.32°, 63.62°, 70.17° and 72.36° at 2θ and indexed to be characteristic 100, 002, 101, 102, 110, 103, 112 and 211 respectively for CdS NPs similar to JCPDS card no # 00-041-1049.

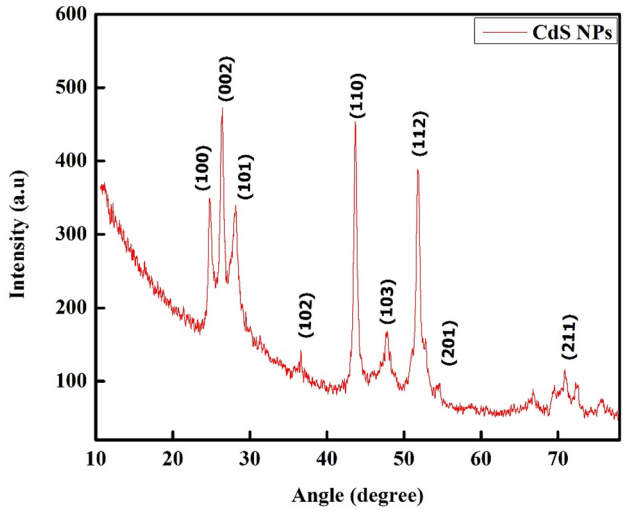

Fig. 4 XRD pattern of CdS nanoparticles

3.3 FTIR Studies

FTIR spectroscopy was used to confirm the purity and to investigate the functional groups of precursors or any other impurities. FTIR spectra were obtained in the range of 500–4000 cm^{-1}. In Fig. 5, the peak at 400–700 cm^{-1} corresponds to the metal-sulfur bond. The peak at 630.33 cm^{-1} corresponds to Cd-S bonding mode and reveals the formation of CdS nanoparticles. The broad peak observed at 3350.67 cm^{-1} was assigned to O–H (hydroxyl group) present because of the moisture absorbed by the CdS NPs. Symmetric C≡C bond mode was observed at 2110.32 cm^{-1} and peak at 1633.54 cm^{-1} was due to asymmetric stretching of C=C bond representing the presence of traces of organic impurities[17].

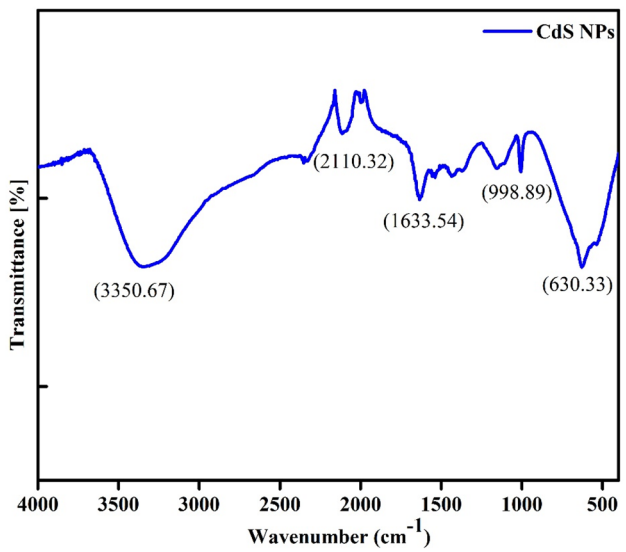

Fig. 5 FTIR spectrum of CdS nanoparticles

3.4 SEM and EDX Studies

The SEM image shown in Fig. 6 with 500 nm magnifications indicates the formation and shape (morphology) of nanoparticles. The grains of particles have aggregated to form just like clusters. The CdS NPs was obtained as fine and uniform particles which produce crystalline aggregates [18]. Energy dispersive X-rays spectroscopy (EDX) was performed for the elemental composition of CdS NPs are shown in Fig. 7. The EDX spectra reveal the presence of Cd and S as major elements in synthetic material and provide the quantitative analysis of weight percentage of compositional elements.

3.5 Thermo Gravimetric Analysis (TGA) of CdS Nanoparticles

TGA was used to study thermal behavior of the prepared CdS. Formation of nano structured materials depends upon temperature and temperature-induced phase changes are significant for the utility of these NPs for various applications [19]. The TGA was carried out under N_2 atmosphere in the temperature range of 25–600 °C at heating rate of a 10 °C min^{-1}. TGA curve of the sample shown in Fig. 8 exhibits that the sample was quite stable to temperature. The weight loss of CdS from 40 to 250 °C, was 4.89% which is due to the presence of water and moisture content present in sample. The weight loss after 250 °C that is mainly assigned to the degradation of the nanomaterials was only 1.65%. The TGA study indicated that the synthesized CdS nanomaterials were much stable to temperature and the total loss occur for 25–600 °C was only 6.54%.

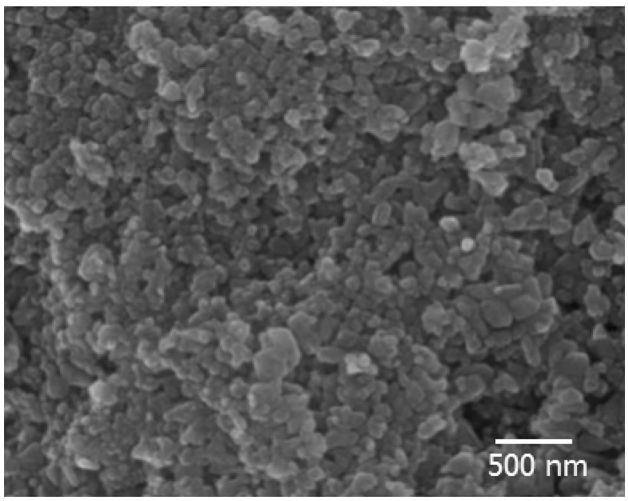

Fig. 6 Scanning electron microscopic image of CdS nanoparticles

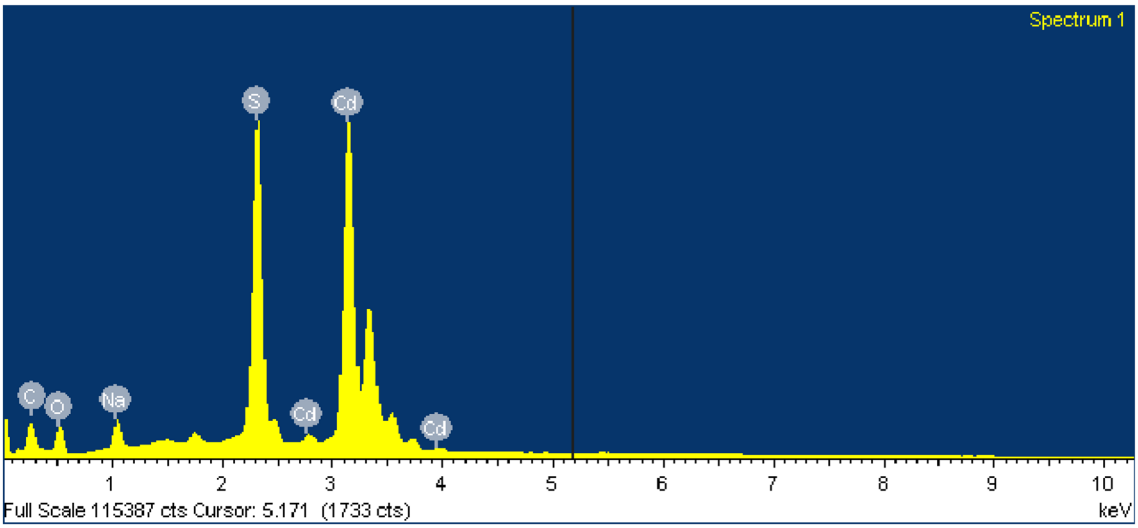

Fig. 7 Energy dispersive X-rays spectrum of CdS nanoparticles

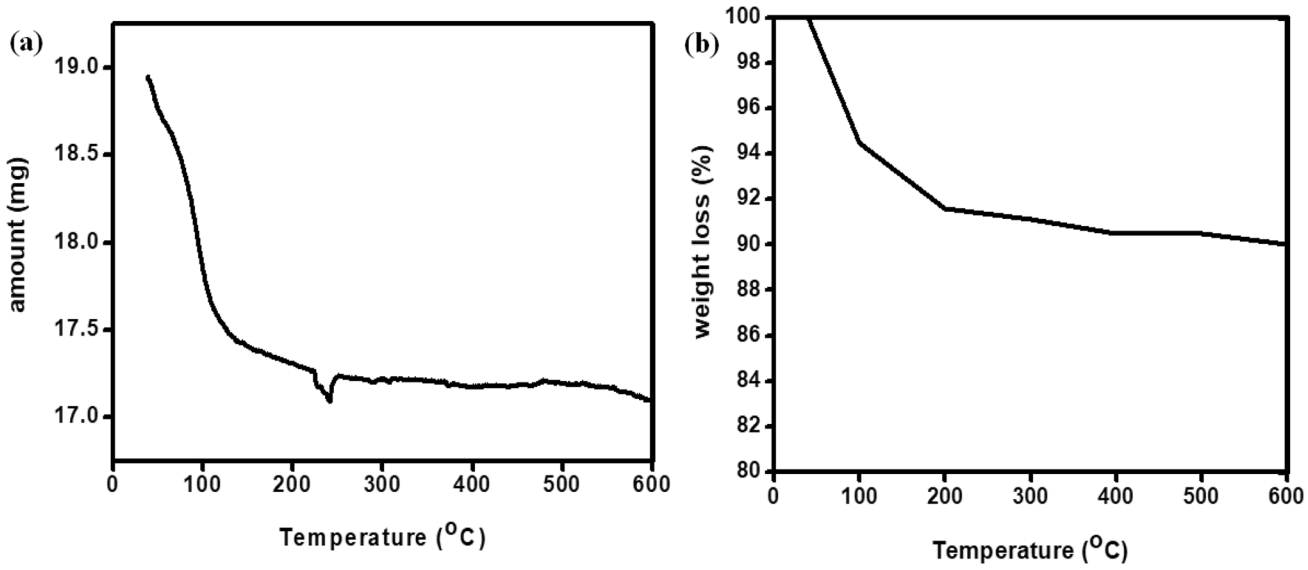

Fig. 8 TGA curve of CdS **a** weight loss in mg and **b** weight loss in percentage

3.6 Photo Degradation Study of Methylene Blue Dye

In the present study CdS NPs were used as photo catalysts for the degradation of methylene blue dye. The following mathematical pseudo first order kinetic model (Eq. 4) was applied to estimate the kinetics of photo degradation of methylene blue dye.

$$-dC/dt = k_{APP}C, \quad (4)$$

where k_{App} denotes rate constant of reaction. The integrated form of the above equation is as

$$\ln(Co/C) = k_{APP}.\ t, \quad (5)$$

where C_o and C represents initial and final degradation of the dye respectively.

Figure 9a, b represent the kinetic analysis for the photo degradation of methylene blue dye. As evident from the Fig. 10 the speed of photo catalytic reaction is powerfully affected by the catalyst identity. The values of k_{App} and correlation coefficient of the pseudo first and second order for

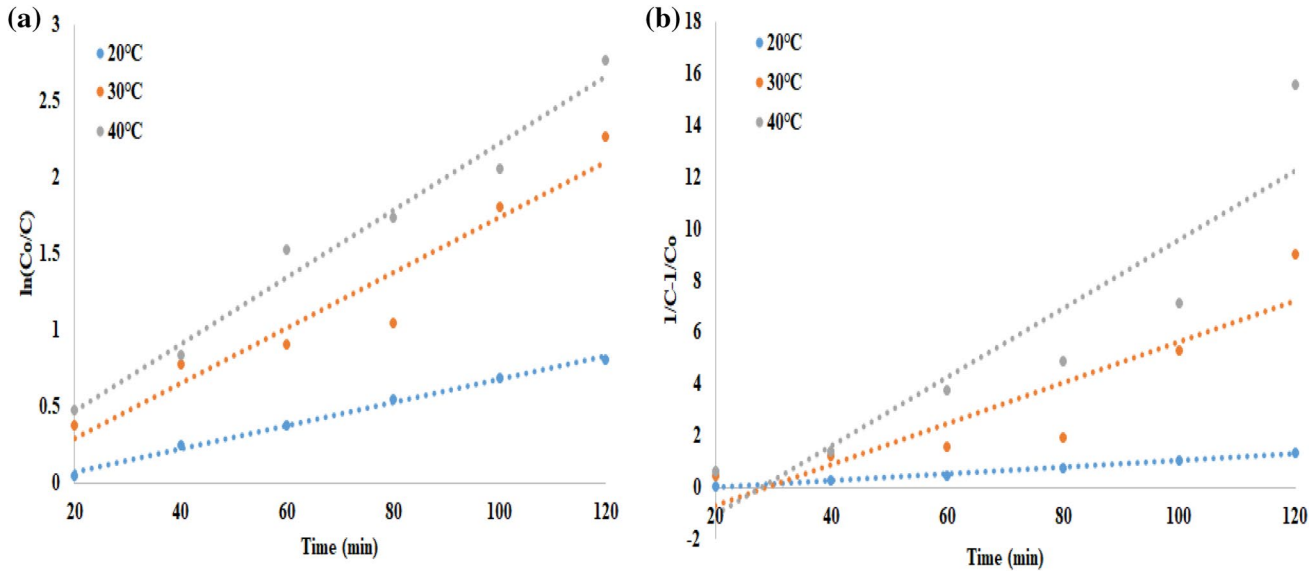

Fig. 9 **a** Application of pseudo first-order kinetics and **b** pseudo second order kinetics to methylene blue dye degradation on CdS NPs at various temperature

the photo degradation reaction of methylene blue dye over CdS NPs are given in Table 1. These kinetic parameters clearly shows that dye interaction with CdS NPs greatly affect catalytic performance. The following pseudo second-order kinetic model (Eq. 6) was applied for the estimation of order of photo degradation of methylene blue over CdS

$$\frac{1}{C} - \frac{1}{C_o} = k_{APP} \cdot t. \tag{6}$$

From the plot it is evident the experimental data best fits the second order model. So the degradation of methylene blue over CdS nanocatalyst follows second order kinetics.

The activation energy of the reaction was calculated using Arrhenius Eq. (7)

$$K = Ae^{\frac{-Ea}{RT}}, \tag{7}$$

where Ea represent activation energy and k represent the rate constant. Logarithmic form of the this equation is the following Eq. (8)

$$\ln k = \ln A - \frac{Ea}{RT}. \tag{8}$$

Plotting lnk vs 1/T a straight line is obtained with a negative slope Ea/R given in Fig. 10. From the given plot the calculated activation energy came out to be 9.043 kJ mol^{-1} as revealed in Table 1.

The effect of dye concentration on the rate of reaction was also studied. A varying concentration (between 10 and 25 mg L^{-1}) of the dye was used. First order and second order rate constant equations were applied to the experimental data for getting apparent rate constants. The plots are shown in Fig. 11a, b. The calculated values of rate constants along with their respective regression coefficients are given in Table 2.

From the data given in Table 2 it is evident that catalytic performance is enhanced with CdS NPs and the experimental data best fits the second order kinetics model.

Table 1 Correlation coefficient along with their k_{App} of the pseudo first and second-order photo degradation reaction of methylene blue dye over CdS NPs

Temperature (°C)		Pseudo-first-order kinetics		Pseudo-second-order kinetics		Activation energy (kJ mol^{-1})
		k_{App}	R^2	k_{App}	R^2	
CdS	20	0.0076	0.9946	0.0126	0.9954	9.043
	30	0.0181	0.9306	0.0793	0.8118	
	40	0.0218	0.9767	0.1333	0.8348	

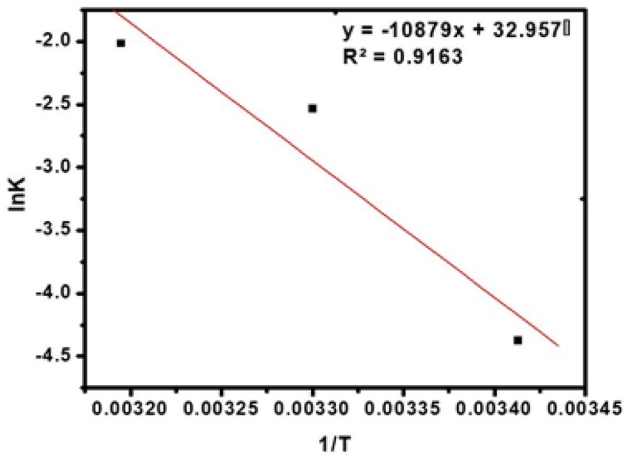

Fig. 10 Plot of Arrhenius equation for the rate constant (k_{App}) of methylene blue dye degradation on CdS NPs

3.7 Mechanism of Photo Catalytic Degradation of Methylene Blue Dye

Photo catalysis usually involves photo-absorption and photo-excitation of electrons from valence band (VB) to the conduction band (CB) of a semiconductor material. Electron–hole formation (Eq. 9), their transfer across the valence, conduction and forbidden energy bands and their recombination has been reported in the photocatalysis on the bases of band gap theory [20].

Upon absorption of higher energy photon an electron is promoted from the VB to the CB (e^-) of CdS with simultaneous generation of a hole (h^+) in the VB. The electrons and holes recombine in the bulk or surface of the particle in a few nano seconds. Trapped energy in the surface sites can react with donor (D) or acceptor (A) species adsorbed or close to the surface of the particle. $OH^{\cdot -}$ radicals are generated when h^+ in VB react with water molecule (Eq. 10) and O_2^- radicals are form by the reaction of electron in CB react with dissolved O_2 molecule (Eq. 11). Complete conversion of an organic substrate to CO_2 and H_2O is carried out by the oxidative pathway as also evident from the mechanism given in Fig. 12 [21].

$$CdS + h\nu\,(\text{light}) \rightarrow e^- + h^+ \tag{9}$$

$$h^+ + H_2O \rightarrow {}^{\cdot}OH + H^+ \tag{10}$$

Table 2 Kinetic constant parameter values for the photo catalytic degradation at different initial concentration of dye

Concentration (ppm)		Pseudo-first-order kinetics		Pseudo-second-order kinetics	
		k_{App}	R^2	k_{App}	R^2
CdS	10	0.0175	0.9403	0.0742	0.6602
	15	0.0095	0.9726	0.0286	0.9114
	20	0.008	0.9665	0.0105	0.8784
	25	0.0062	0.9751	0.004	0.9589

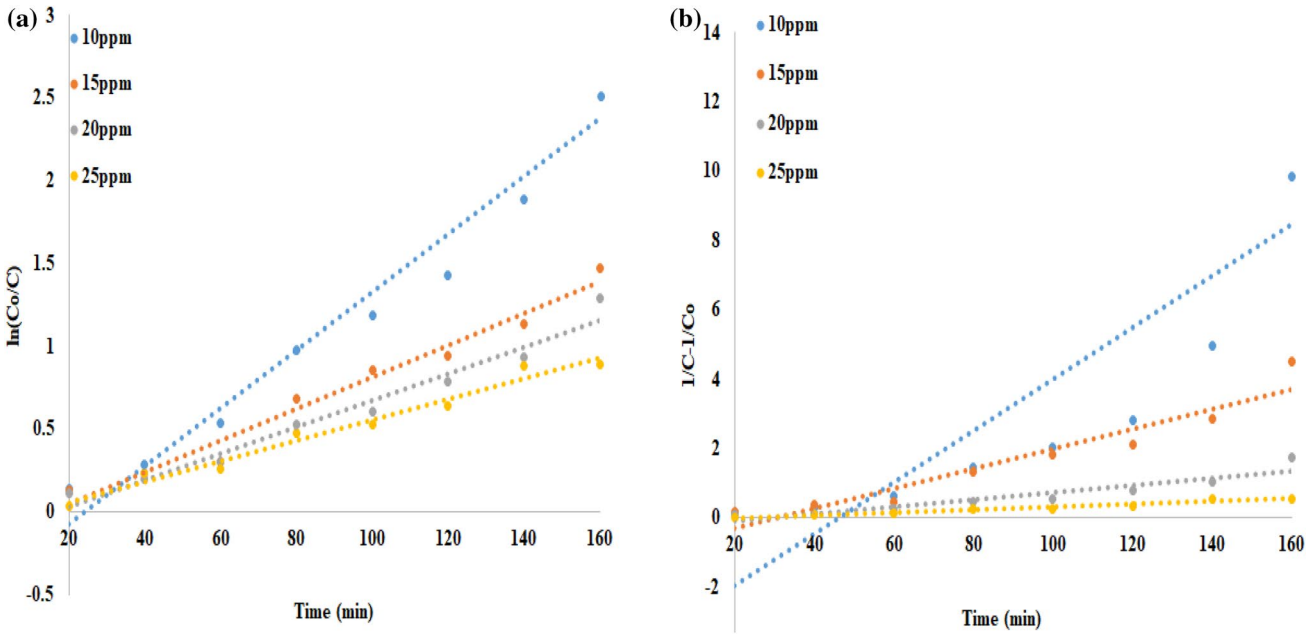

Fig. 11 **a** Application of pseudo first-order kinetics and **b** pseudo second order kinetics to methylene blue dye degradation on CdS NPs at various initial concentration

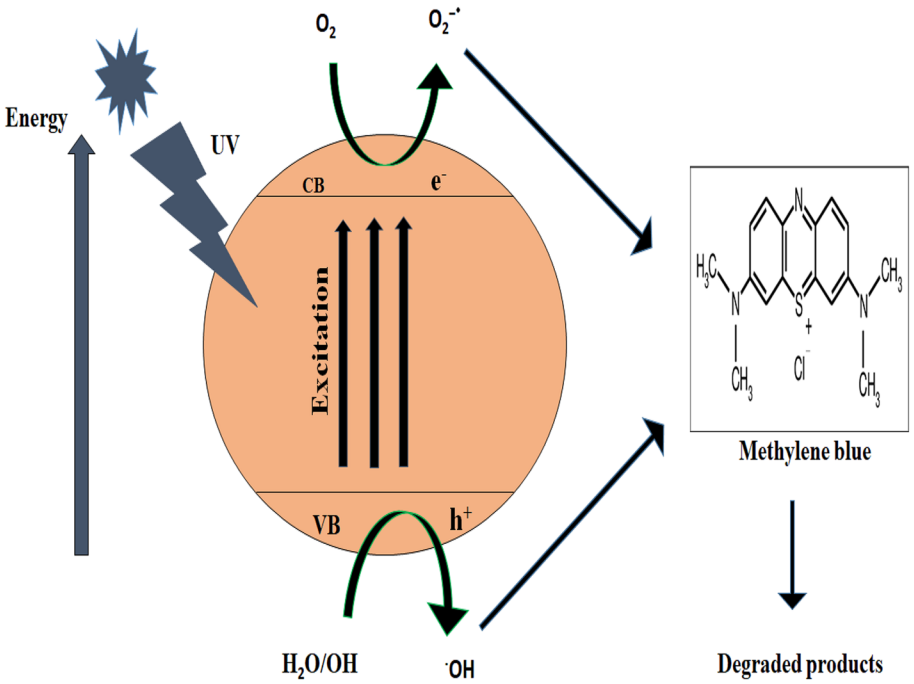

Fig. 12 Mechanism of possible photo catalytic degradation of methylene blue dye

$$e^- + O_2 \rightarrow {}^{\cdot} O_2^- \quad (11)$$

OH + dye molecules → degraded products

O_2^- + dye molecules → degraded products.

3.8 Effect of Time and Concentration on Dye Degradation

Irradiating under UV light 10, 15, 20 and 25 ppm concentration of dye upon addition of 0.03 g of photocatalyst (CdS) the changes in percent degradation of MB dye different time intervals are shown in Fig. 13. It is evident from the plots that degradation increases with increase in time duration. The photo degradation efficiency of CdS for degradation at each experimental concentration of MB after a time interval of 160 min was found to be 93.8%, 77%, 72% and 59% respectively. Due to more active sites for MB molecules to be adsorbed on the surface of CdS photo-catalyst the data indicated that degradation is higher at lower concentration. With increase in concentration of dye the number of dye molecules adsorbed on catalyst surface increases. Owing to this high concentration of the molecules needed to absorb light photons and to subsequently reach the catalyst surface decreases and lead to reduction in efficiency of photo catalyst [22, 23]. Thus better degradation of MB dye was achieved at 10 ppm.

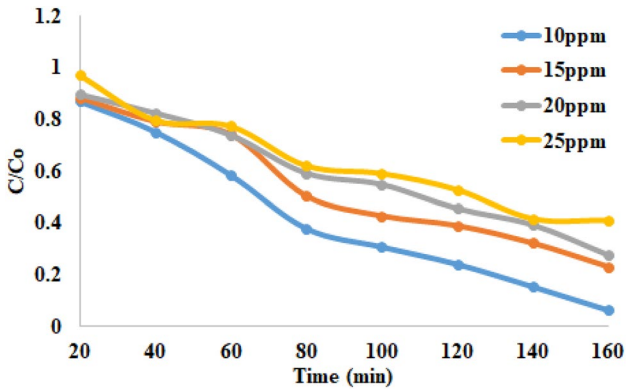

Fig. 13 Effect of CdS NPs on methylene blue dye degradation at various initial concentration

3.9 Effect of Temperature on Dye Degradation

The effect of temperature on methylene blue degradation in aqueous solutions in the presence of CdS was studied at various temperatures i.e. 20, 30 and 40 °C the plot is given in Fig. 14. An increase in percent degradation of MB dye was observed with increase in temperature. Percent degradation for each temperature calculated was 55, 89 and 93 respectively. In the present work it was recorded that rise in temperature not only increased percent degradation, but also the rate of reaction. This phenomenon might be explained in term of $^{\cdot}OH$ generation as a function of temperature. It was suggested that the rise in temperature accelerates the reaction between H_2O and CdS, hence the generation of oxidizing species like $^{\cdot}OH$ radical become improved [24, 25].

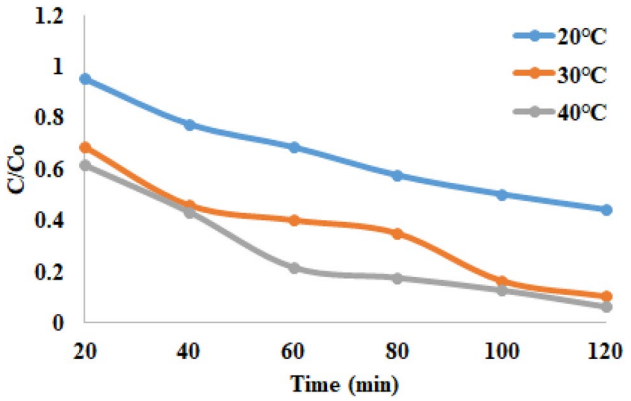

Fig. 14 Effect of CdS NPs on methylene blue dye degradation at different temperature

3.10 Effect of Photo Catalyst Dosage on Dye Degradation

By changing the catalysts CdS mass from 0.01 to 0.05 g for 140 min illumination under UV light the effect of the catalyst dose on the dye degradation was investigated as shown in Fig. 15a, b. The percent degradation calculated for each dose is also given in Table 3. With increase in CdS photo catalyst mass from 0.01 to 0.03 g an increase in dye degradation was observed. The increase in mass of the catalyst contributed to an increased surface resulting in more photons received at the surface of catalysts. The degradation of dye

Table 3 Photo catalytic degradation of methylene blue dye at different amount of CdS NPs

Catalyst mass (g)	0.01	0.02	0.03	0.04	0.05
Degradation (%)	89	91.1	96.6	93	91.1

was 89% using 0.01 g of the catalyst which got increased to 96% at 0.03 g. By further increasing the photo catalyst mass a slight decline in percent degradation of MB was observed i.e. at 0.05 g the percent degradation decreased to 91%. This can be attributed to the fact that with increase in catalyst loading the number of active sites may increases but the penetration of light decreases due to shielding effect as well as owing to deactivation of activated molecules by collision with ground state catalysts reduces the rate of reaction [26].

3.11 Effect of pH on dye degradation

During the degradation process the electrostatic interaction between substrates, catalyst surfaces and radicals is determined by the pH of wastewater containing dye. Surface charge and aggregation of the catalysts is also affected by pH [27]. The effect of pH of the medium on the photo catalytic degradation of methylene blue was investigated by carrying out the experiment at pH range of 4–9 while keeping other parameters constant. As evident from Fig. 16 and Table 4 a gentle rise in the reaction rate was observed when pH increased from 3 to 9. This confirms the sensitivity of

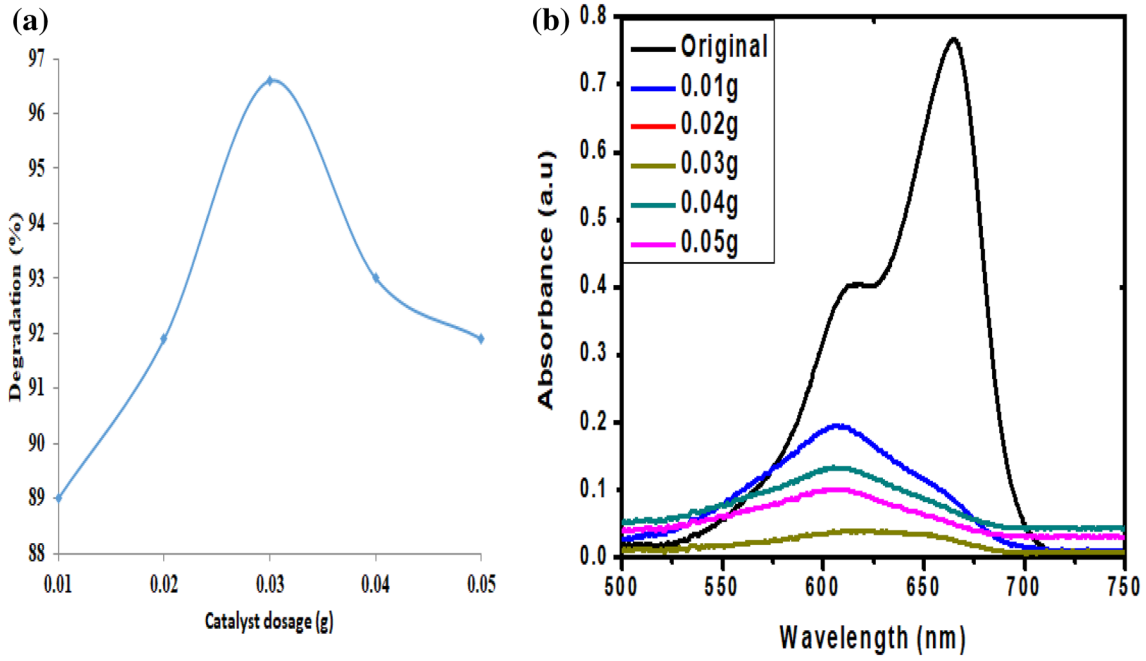

Fig. 15 Percent degradation of methylene blue dye using different mass of CdS NPs. **b** UV visible spectra at different catalyst dosage

MB dye degradation to the pH of the reaction mixture. This can be attributed to the fact that pH not only influences the surface state of catalyst but also ionization state of ionizable organic molecules. Thus the pH of the solution directly influences heterogeneous photo catalytic process. In basic medium the high degradation of MB dye might be due to the enhanced formation of hydroxyl radicals. The principal oxidizing species at high pH conditions are hydroxyl radicals which are responsible for degradation of organic dye [28]. Conversely in acidic conditions CdS particles agglomerate, leading to a reduced exposed surface area to the energy source (UV-light) [29]. Electrostatic attraction between dye molecules and the surface of CdS is promoted in alkaline pH, this is why high photo catalytic degradation of MB was achieved at pH 9 [30].

3.12 Catalyst Stability Study

In large-scale processes the stability of photo catalyst is important that's why the recyclability and stability of the CdS photo catalyst was also investigated through the degradation of MB under UV light. Through centrifugation the catalyst was recycled and then washing with ethanol followed by twice with deionized water and drying at 50 °C for 30 min without any additional treatment and was then reused for subsequent degradation. Figure 17 and Table 5 depicts slight decline in the efficiency of recovered catalyst as compare to the original, which may be attributed to deactivation of the catalyst in the cycling experiment and little loss. The catalyst could be stated to have high stability and durability [31].

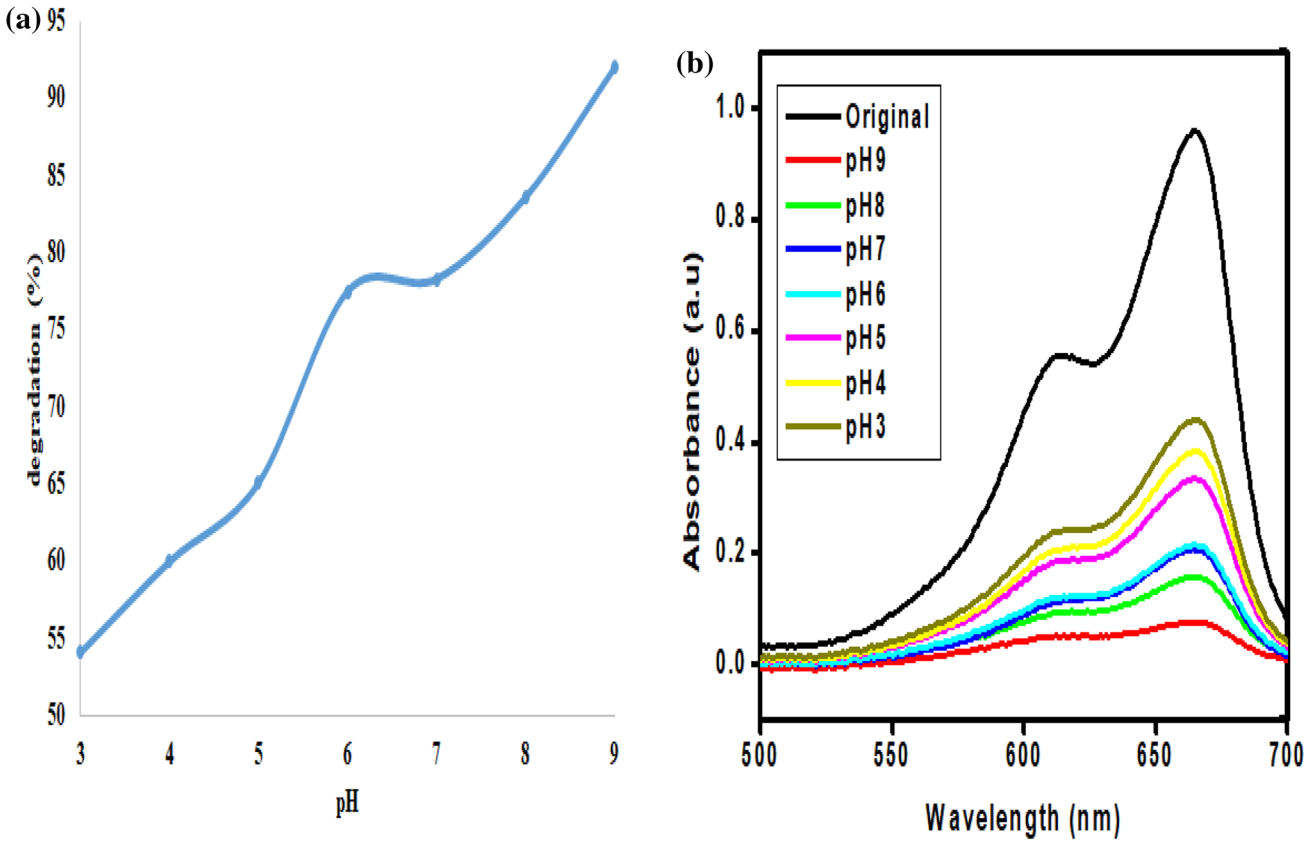

Fig. 16 **a** Percent degradation of methylene blue dye at different pH. **b** UV visible spectra at different pH

Table 4 Percent degradation of methylene blue dye at different pH

pH value	3	4	5	6	7	8	9
Degradation (%)	54.1	60	65	75	78	83.6	92

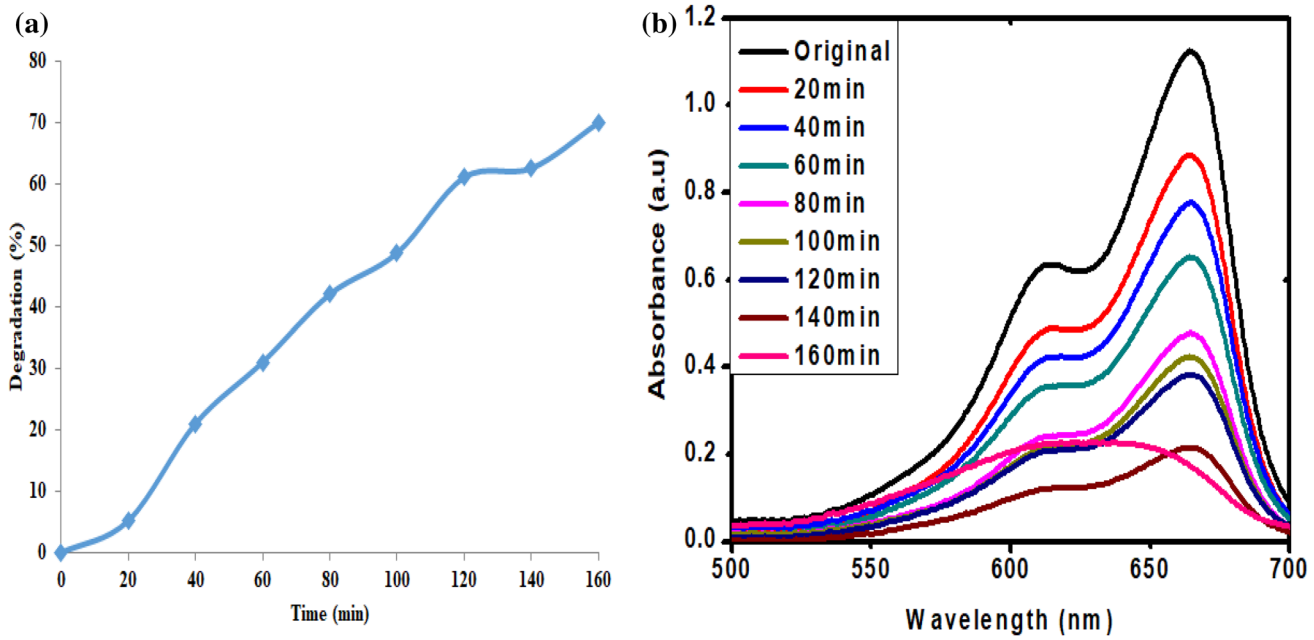

Fig. 17 **a** Percent degradation of methylene blue dye on recycled CdS NPs. **b** UV visible spectra at different time interval

Table 5 Percent degradation of methylene blue dye using recycled CdS NPs

Time (min)	20	40	60	80	100	120	140	160
Degradation (%)	5	21	31	42	62	67	80	84.7

4 Conclusions

The successfully synthesized CdS through hydrothermal route have a band gap of 2.38 eV. The particles were aggregated to form clusters with crystalline hexagonal structures. CdS nanoparticles were found to be very stable to temperature as a small loss (6.54%) in weight occurred during heating 25–600°C.About 94% dye degradation was noticed at 160 min time duration. The dye degradation was found to decrease with increase in the initial concentration of dye. Increasing the temperature up to 40 °C and pH up to 9 of the medium the degradation was found to increase. The degradation of MB over CdS catalyst surface follows second order kinetics. The calculated activation energy of the photo catalysis was 9.043 kJ mol^{-1}. The recyclability study showed that the CdS are stable and durable nanoparticles.

References

1. Salama A, Mohamed A, Aboamera NM, Osman TA, Khattab A (2018) Photocatalytic degradation of organic dyes using composite nanofibers under UV irradiation. Appl Nanosci 8:155–161
2. Khairnar SD, Shrivastava VS (2019) Facile synthesis of nickel oxide nanoparticles for the degradation of methylene blue and Rhodamine B dye: a comparative study. J Taibah Univ Sci 13:1108–1118
3. Arques A, Amat AM, Garcia-Ripoll A, Vicente R (2007) Detoxifcation and/or increase of the biodegradability of aqueous solutions of dimethoate by means of solar photocatalysis. J Hazard Mater 146:447–452
4. Khan A, Valicsek Z, Horváth O (2020) Synthesis, characterization and application of iron(II) doped copper ferrites (CuII(x) FeII(1−x)FeIII 2O4) as novel heterogeneous photo-Fenton catalysts. Nanomater 10:921
5. Kaur J, Sharma M, Pandey OP (2014) Synthesis, characterization, photocatalytic and reusability studies of capped ZnS nanoparticles. Bull Mater Sci 37:931–940
6. Hasani K, Peyghami A, Moharrami A, Vosoughi M, Dargahi A (2020) The efficacy of sono-electro-Fenton process for removal of Cefixime antibiotic from aqueous solutions by response surface methodology (RSM) and evaluation of toxicity of effluent by microorganisms. Arab J Chem 13:6122–6139
7. Sirés I, Brillas E, Oturan MA, Rodrigo MA, Panizza M (2014) Electrochemical advanced oxidation processes: today and tomorrow. A review. Environ Sci Pollut Res 21:8336–8367
8. Aponte ÁG, Ramírez MAL, Mora YC, Santa Marín JF, Sierra RB (2020) Cerium oxide nanoparticles for color removal of indigo carmine and methylene blue solutions. AIMS Mater Sci 7:468–485

9. Singh A, Goyal V, Singh J, Rawat M (2020) Structural, morphological, optical and photocatalytic properties of green synthesized TiO2 NPs. Curr Res Green Sustain Chem 3:100033
10. Xu J, Avellan A, Li H, Liu X, Noël V, Lou Z, Lowry GV (2020) Sulfur loading and speciation control the hydrophobicity, electron transfer, reactivity, and selectivity of sulfidized nanoscale zerovalent iron. Adv Mater 32(17):1906910
11. Li H, Yang W, Wu C, Xu J (2021) Origin of the hydrophobicity of sulfur-containing iron surfaces. Phys Chem Chem Phys 23:13971–13976
12. Cao Z, Li H, Lowry GV, Shi X, Pan X, Xu X, Xu J (2021) Unveiling the role of sulfur in rapid defluorination of florfenicol by sulfidized nanoscale zero-valent iron in water under ambient conditions. Environ Sci Technol 55(4):2628–2638
13. Venkatesh N, Sabarish K, Murugadoss G, Thangamuthu R, Sakthivel P (2020) Visible light-driven photocatalytic dye degradation under natural sunlight using Sn-doped CdS nanoparticles. Environ Sci Pollut Res 27:43212–43222
14. Rafati AA, Borujeni ARA, Najafi M, Bagheri A (2011) Ultrasonic/surfactant assisted of CdS nano hollow sphere synthesis and characterization. Mater Character 62:94–98
15. Imran M, Ikram M, Shahzadi A, Dilpazir S, Khan H, Shahzadi I, Huang Y (2018) High-performance solution-based CdS-conjugated hybrid polymer solar cells. RSC Adv 8:18051–18058
16. Devendran P, Alagesan T, Pandian K (2013) Single pot microwave synthesis of CdS nanoparticles in ionic liquid and their photocatalytic application. Asian J Chem 25(Supplementary Issue):S79
17. Mahdi HS, Parveen A, Azam A (2017) Microstructural and optical properties of sol gel synthesized CdS nano particles using CTAB as a surfactant. In: AIP conference Proceedings 2017. AIP Publishing LLC
18. Ayodhya D, Veerabhadram G (2019) Facile fabrication, characterization and efficient photocatalytic activity of surfactant free ZnS, CdS and CuS nanoparticles. J Sci Adv Mater Dev 4:381–391
19. Alipour A, Lakouraj MM, Tashakkorian H (2021) Study of the effect of band gap and photoluminescence on biological properties of polyaniline/CdS QD nanocomposites based on natural polymer. Sci Rep 11:1–15
20. Faisal S, Khan MA, Jan H, Shah SA, Shah S, Rizwan M, Akbar MT (2020) Edible mushroom (Flammulina velutipes) as biosource for silver nanoparticles: from synthesis to diverse biomedical and environmental applications. Nanotechnology 32(6):065101
21. Saeed K, Khan I, Sadiq M (2016) Synthesis of graphene-supported bimetallic nanoparticles for the sunlight photodegradation of Basic Green 5 dye in aqueous medium. Sep Sci Technol 51:1421–1426
22. Ming LY (2000) Treatment of dye aqueous solution by UV/TiO_2 process with applying bias potential. Water Sci 36:189–106
23. Alkaykh S, Mbarek A, Ali-Shattle EEX (2000) Photocatalytic degradation of methylene blue dye in aqueous solution by $MnTiO_3$ nanoparticles under sunlight irradiation. Heliyon. 6(4):e03663
24. Sun J, Sun S, Wan G, Qiao L (2007) Degradation of azo dye amido black 10B in aqueous solution by Fenton oxidation process. Dye Pigment 74:647–652
25. Khan J, Tariq M, Muhammad M, Mehmood MH, Ullah I, Raziq A, Niaz A (2019) Kinetic and thermodynamic study of oxidative degradation of acid yellow 17 dye by Fenton-like process: effect of HCO^{3-}, CO_3^{2-}, Cl^- and SO_4^{2-} on dye degradation. Bull Chem Soc Ethiop 33:243–254
26. Jamal N, Radhakrishnan A, Raghavan R, Bhaskaran B (2020) Efficient photocatalytic degradation of organic dye from aqueous solutions over zinc oxide incorporated nanocellulose under visible light irradiation. Main Group Metal Chem 43:84–91
27. Anwer H, Mahmood A, Lee J, Kim KH, Park JW, Yip AC (2019) Photocatalysts for degradation of dyes in industrial effluents: opportunities and challenges. Nano Res 12:955–972
28. Shah T, Gul T, Saeed K (2019) Photodegradation of bromophenol blue in aqueous medium using graphene nanoplates-supported TiO_2. Appl Water Sci 9(4):105
29. Mortazavian S, Saber A, James DE (2019) Optimization of photocatalytic degradation of acid blue 113 and acid red 88 textile dyes in a UV-C/TiO_2 suspension system: application of response surface methodology (RSM). Catalysts 9:360
30. Hamza M, Altaf AA, Kausar S, Murtaza S, Rasool N, Gul R, Zakaria ZA (2020) Catalytic removal of alizarin red using chromium manganese oxide nanorods: degradation and kinetic studies. Catalysts 10:1150
31. Chen X, Wu Z, Liu D, Gao Z (2017) Preparation of ZnO photocatalyst for the efficient and rapid photocatalytic degradation of azo dyes. Nanoscale Res Lett 12:143